ABSTRACT
This document provides the technical final report for the ESA-funded lunar project

Emma Woolliams
Sarah Taylor
Carlos Toledano
Stefan Adriaensen
Africa Barreto
Alberto Berjón

NPL, VITO, UVa

08 December 2019

EXECUTIVE SUMMARY

Signatures and version history

	Name	Organisation	Date
Written by	Sarah Taylor	NPL	08 December 2019
Reviewed by (consortium)	Emma Woolliams	NPL	08 December 2019
Approved by (ESA)	Marc Bouvet	ESA	17 December 2019

Version history

Version	Date	Publicly available or private to consortium?
0.1	8/12/2019	Public

Contents

1 Introduction

1.2 Purpose and Scope

This document provides the final report for the ESA-funded project "Lunar spectral irradiance measurement and modelling for absolute calibration of EO optical sensors" under ESA contract number: 4000121576/17/NL/AF/hh

1.3 Applicable and reference documents

1.3.1 Applicable Documents

The following applicable documents are those specification, standards, criteria, etc. used to define the requirements of this representative task order.

Number	Reference
[AD0]	ESA-TECEEP-SOW-002720. Lunar spectral irradiance measurement and modelling for absolute calibration of EO optical sensors.
[AD1]	Deliverable-1: Strategy for the derivation of an improved lunar spectral irradiance model based on lunar photometer measurements
[AD2]	Deliverable-2: Lunar spectral irradiance measurement protocol from a lunar photometer
[AD3]	Deliverable-3: Lunar photometer calibration for lunar spectral irradiance measurements
[AD4]	Deliverable-4: Lunar spectral irradiance measurement uncertainties from a lunar photometer
[AD6]	Deliverable-5: Operation and maintenance manual for lunar photometer
[AD6]	Deliverable-6: Lunar spectral irradiance retrieval from the lunar photometer measurements
[AD7]	Deliverable-7: Lunar irradiance model algorithm and theoretical basis document
[AD8]	Deliverable-8: Comparison of lunar irradiance model with several datasets

executive summary

1.4 Glossary

1.4.1 Abbreviations

Abbreviation	Stands For	Notes
ESA	European Space Agency	Project customer
NPL	National Physical Laboratory	Project partner
UVa	University of Valladolid	Project partner
VITO	Vlaamse Instelling voor Technologisch Onderzoek; Flemish Institute for Technological Research	Project partner
USGS	U. S. Geological Survey	
VNIR	Visual and Near InfraRed	
SWIR	Short-Wave InfraRed	
DOLP	Degree of linear polarisation	

2 Project executive summary

Satellite Earth Observation provides essential data sets for a wide range of commercial, societal and scientific applications. Satellites have been observing the state of the environment since the launch of the radiation balance instrument on Explorer 8 in October 1959, and over the last 60 years the range of observation types and applications has grown exponentially. Today operational long-term sustained Earth Observation programmes, exemplified by the Copernicus Sentinels, give a wide range of users reliable environmental information services. These EO data will also provide a legacy of information about environmental and climate change for future generations seeking to manage their collective existence within the environments of Earth.

To meet the interoperability demands of today's applications, which combine data from different sensors, and to meet the long-term stability requirements of climate change analyses that must observe small trends on top of large natural variability, satellite data sets must be stable, harmonised, and have associated with them reliable and robust evaluations of their uncertainty. Recognising this the Committee on Earth Observation Satellites (CEOS) agreed a "Quality Assurance Framework for Earth Observation" (QA4EO; www.qa4eo.org) in 2010, which set guidelines for establishing and providing quality indicators for satellite sensor data records.

Vicarious calibration and comparison methods, which use observations of reference sites to monitor the stability and/or absolute performance of satellite instruments, as well as to determine inter-sensor biases, have long been used to evaluate the performance of Earth Observation sensors. These references include natural phenomena (e.g. Rayleigh scattering over dark ocean sites, sun-glint reflected from water, deep convective clouds which provide a "white" reference for inter-band calibration), pseudo-invariant calibration sites (PICS), such as those in deserts or ice sheets that are sufficiently stable over time for non-simultaneous sensor inter-comparisons and for long-term stability monitoring, and instrumented sites such as the radiometric calibration network RadCalNet.

One important vicarious reference source is the Moon. With no atmosphere, the Moon is extremely stable long term. Geostationary satellite instruments sometimes observe the Moon in the "dark space corners" of the image and low earth orbit sensors can be manoeuvred to observe the Moon. Many satellites already use the Moon as a calibration source, particularly to monitor long term stability. The Moon also has a similar reflectance to the earth, and so calibrates sensors at the correct level (unlike, say, very bright targets such as clouds and onboard calibration references).

However, to use the Moon as a reference, it is necessary to model the phase and libration changes in the Moon. There are many periodic cycles that apply to the Moon, Earth and Sun geometry. The cycle with the longest period is called the Saros cycle and its duration is 223 synodic months, which is 18 years, 11 days and 8 hours. After this cycle, Earth, Moon and Sun return to the same relative geometry. The shortest cycle is the variation in phase angle which takes about 28 days between two full moons. The cycle for the distance between Sun and Earth/Moon takes about one year.

Current lunar observations are corrected for this cycle using the ROLO model, or the GSICS implementation of the ROLO model (GIRO). The ROLO (Robotic Lunar Observatory) model is based on observations made between March 1996 and September 2003 by Kieffer and Stone [RD1] which are fitted to a model described by

$$\ln(A_k) = \sum_{i=0}^{3} a_{ik} g^i + \sum_{i=1}^{3} b_{ik} \Phi^{2i-1} + c_{1k}\theta + c_{2k}\phi + c_{3k}\Phi\theta + c_{4k}\Phi\phi + d_{1k}e^{-\frac{g}{p_1}} + d_{2k}e^{-\frac{g}{p_2}}$$
$$+ d_{3k}\cos\left(\frac{g - p_3}{p_4}\right)$$

Here, the natural logarithm of the lunar reflectance for a wavelength λ_k is modelled

- as a third order polynomial (the a_{ik} term) of phase angle, g,
- the b_{ik} terms consider the change in reflectance with phase angle (due to variations in the Maria and Highlands across the disk)
- the c_{ik} terms consider the topographic libration (the part of the lunar disk that is visible): and finally the d_{ik} terms are empirically-fitted terms that explain variation from this physical model

This project aimed to determine an improved model based on the same equation, but with new lunar observations and to compare this improved model with the original ROLO/GIRO model and with satellite observations of the Moon. The project involved the following steps:

First, in Task 1, a measurement strategy was defined. This involved considering choices for the instrument: a multispectral "sun photometer" was chosen, from CIMEL of type 318-TP9. This type had been modified to cover the necessary dynamic range to observe the Moon as well as the Sun and is therefore known as a "lunar photometer". We chose a multispectral instrument, rather than a hyperspectral instrument, for the improved dynamic range and an instrument that had polarization capability as the lunar polarization is known to change with phase angle.

The measurement strategy chosen was to use the lunar photometer to obtain "night Langleys". A Langley plot is commonly used to measure atmospheric aerosol thickness. The principle is that the Sun (day) or Moon (night) is observed continuously over a 2-3 hour period during which it rises or sets. As the Sun/Moon rises or sets, the observation passes through an increasing (or decreasing) air mass, and, if the aerosol optical thickness is stable during the period of the Langley, the measured signal will change. Beer's law states that for each instantaneous measurement, the direct-Sun irradiance (as measured through the atmosphere), E_t is linked to the solar extraterrestrial irradiance E_0 and the atmospheric optical depth τ by:

$$\frac{E_t}{E_0} = e^{-m\tau}.$$

where m is the airmass factor. Therefore, by taking natural logarithms of both sides of this equation, we can see that a plot of $\ln(E_t)$ as a function of airmass m is a straight line with a slope of $-\tau$ and an intercept of $\ln(E_0)$. This method is usually used to obtain the aerosol optical thickness (one component of the atmospheric optical depth), but by taking measurements at a site with very low and very stable aerosol levels, it can be used to measure the lunar extra-atmospheric irradiance.

The CIMEL 318-TP9 instrument was purchased and then, also in Task 1, calibrated and characterized at the National Physical Laboratory, the United Kingdom's national metrology institute, against SI-traceable standards. This required a specialist set up in order to match lunar irradiance levels whilst ensuring the source was sufficiently small to be fully within the field-of-view of the instrument. The standard uncertainty associated with the calibrated irradiance responsivity of the instrument after calibration was between 0.91 % and 1.06 % for wavelengths from 440 nm to 1640 nm. (Expanded uncertainty at the 95 % confidence level, for $k = 2$, were between 1.8 % and 2.1 %). The instrument was also characterized for temperature-sensitivity at the University of Valladolid's facility. This is important, as operational temperatures vary considerably during outdoor operation in both nighttime and daytime.

executive summary

Figure 1: Laboratory set up at NPL for the radiometric calibration of the lunar photometer.

After calibration, in Task 2 in March 2018 the lunar photometer was installed on Teide Peak in Tenerife. This location was chosen to meet the requirements for good Langley plots: a stable atmospheric transmittance, an absence of clouds and low aerosol levels. Since aerosols tend to be more concentrated at low altitude below inversions and near large human settlements, Langley extrapolation is usually performed at high, remote, mountain sites. Teide Peak in Tenerife benefits from subsiding air from the descending branch of the Hadley cell. This creates a temperature inversion layer normally located at 800 m – 1500 m preventing the ingress of pollutants from lower parts of the island, thus allowing high quality atmospheric observations to be obtained from this location under free-tropospheric conditions. In the winter months, the lunar photometer was moved to a slightly lower location to avoid hazardous conditions.
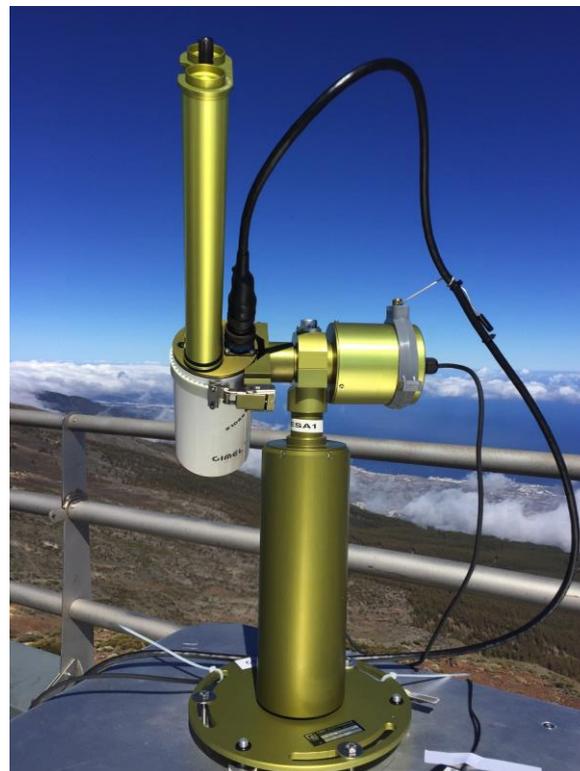

Figure 2: the ESA CIMEL in situ at Izaña Atmospheric Observatory

Task 3 involved the instrument making measurements for the remaining duration of the project on all nights from the end of the first quarter of the lunar phase to the end of the third quarter.

Measurements are taken when the Sun is set (when the solar zenith angle (sun_zenith) is larger than 98°, i.e. optical_air_mass about -7 and the Moon zenith angle (moon_zenith) is below 82°, i.e. air mass below 7) to avoid solar contamination in the observations. Solar Langleys during the daytime were used to monitor instrument stability.

Lunar data are corrected for instrument temperature variations and an iterative procedure established: first the raw data are used to fit Langley straight lines and identify the extra-atmospheric lunar irradiance. Second, these data are used to fit a version of the ROLO model. This fit is then filtered to remove outlier observations, and then the raw data are corrected according to this model to account for lunar phase changes during the Langley plot. With filtered and corrected data, the Langley straight line fit is repeated, a new model is established and then an improved filter and correction is performed. The Langley data provided at the end of this third iteration are stored as project lunar irradiance data.

In Task 4, the lunar irradiance data were used in a more complete fitting process to obtain a lunar model at the wavelengths of the lunar photometer. These data were spectrally interpolated using the same Apollo-sample based spectral reflectance model used in the original ROLO model, and a polarization model was obtained, based on the CIMEL 318-TP9 polarization data. Uncertainties for this model were estimated using Monte Carlo Uncertainty Evaluation based on the calibration uncertainties and the observed variability in the Langley plots (estimated from the χ^2 test on the Langley fit). Overall expanded uncertainties are around 2 %.
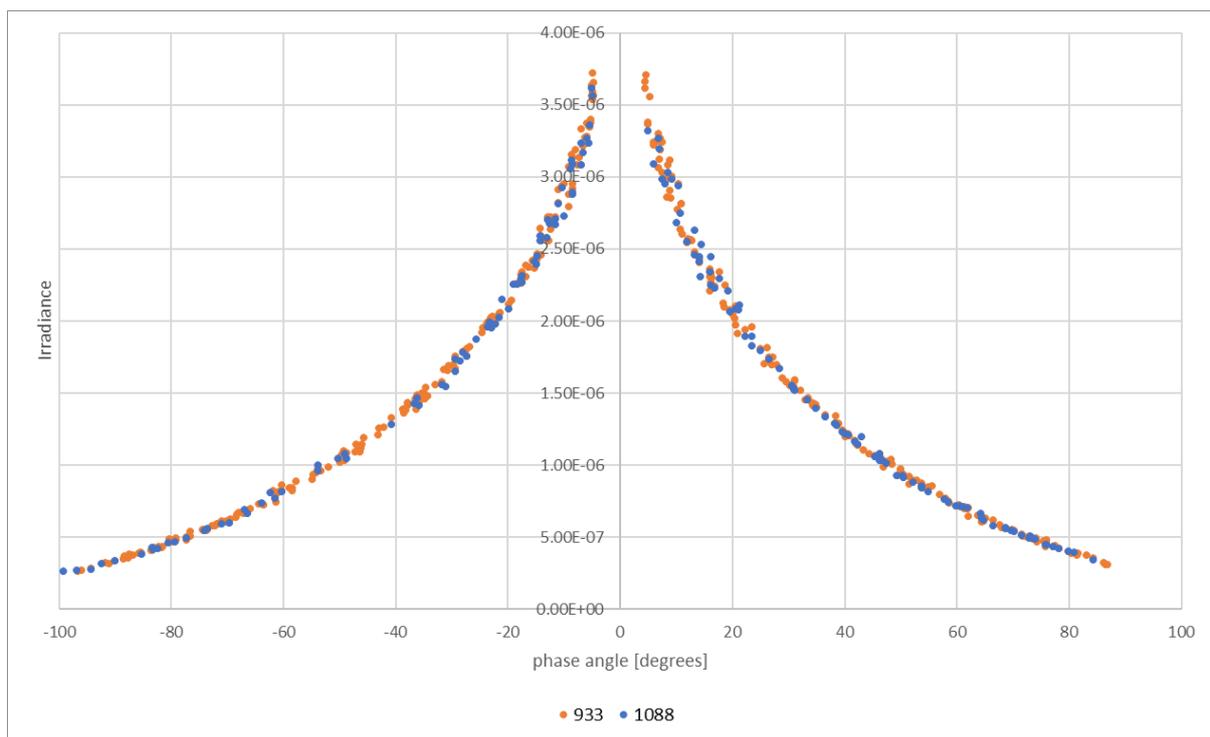

Figure 3:Lunar irradiance measurements for 440 nm from the 1088 and 933 instruments
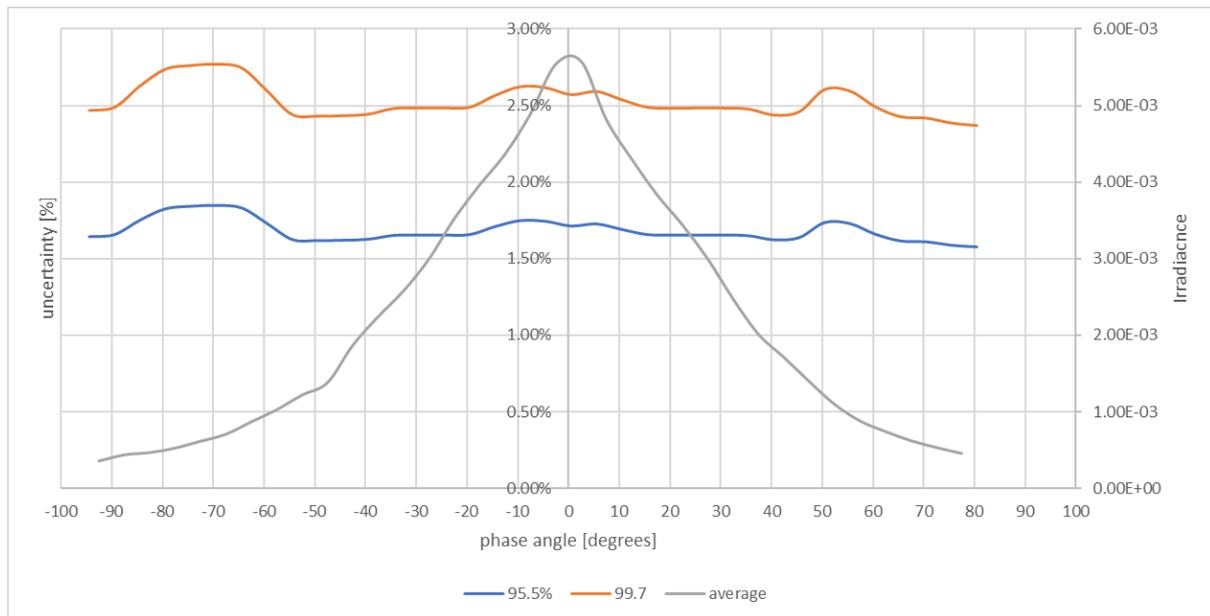
executive summary

Figure 4: Uncertainty levels for the 675 nm band

Finally, in Task 5, the model results were compared with the GIRO model and also with observations of the Moon's irradiance made by the Proba-V sensor (which has a long term record of lunar observations, but always at the same phase – the Moon was observed once a month) and the PLEIADES sensor (with data over a shorter time period, but for more phases). In general, the data agreed better with the satellite sensors than the GIRO model, though there is not yet enough data to draw a firm conclusion.
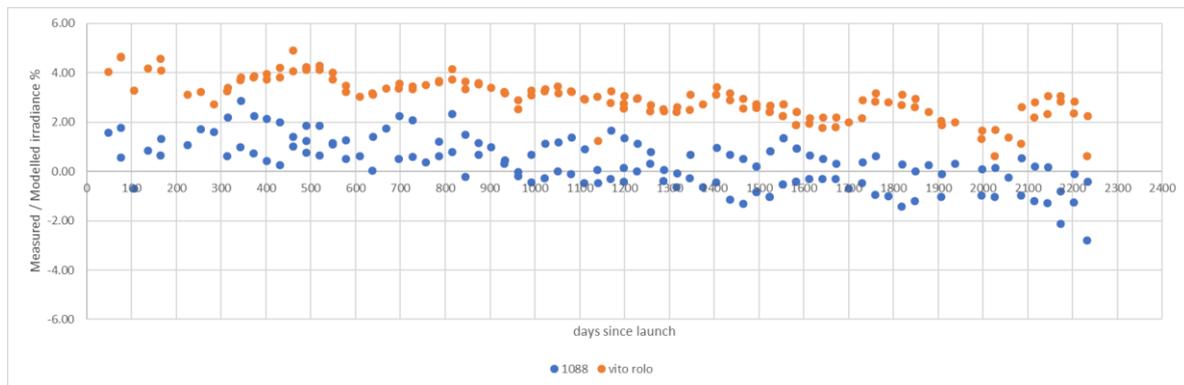

Figure 5: PROBA-V BLUE irradiance compared to the 1088 lunar model

The project has successfully established a new instrument for high quality measurements of the lunar extra-atmospheric irradiance. The instrument was calibrated at a national metrology institute against SI-traceable standards and installed in a location with extremely low aerosol levels and very stable atmospheric conditions. It has operated since March 2018. The data collected so far has been analysed to create a lunar model that has been compared with satellite sensors and shows promise.

It is intended that the work will continue with follow-on projects to continue observing the Moon with the instrument and to continue upgrading the lunar model, both with new measurement data and with an improved spectral interpolation (based on spectral measurements with the hyperspectral Pandora instruments). The model analysis will also be improved using an improved fitting algorithm that is weighted according to the uncertainty associated with the individual Langley plot fits.

Output Deliverables		
D1	Strategy for the derivation of an improved lunar spectral irradiance model based on lunar photometer measurements	40-page PDF giving detailed information on the concepts behind the project, the history of lunar irradiance measurements and models and "ideal" and "practical" options for measuring lunar irradiance
D2	Lunar spectral irradiance measurement protocol from a lunar photometer.	10-page PDF defining the detailed measurement protocol for the observations in the field.
D3	Lunar photometer calibration for lunar spectral irradiance measurements	40-page PDF describing the process for calibrating the lunar photometer's irradiance responsivity, and also giving the results of the temperature sensitivity characterisation.
D4	Lunar spectral irradiance measurement uncertainties from a lunar photometer	55-page PDF giving a full uncertainty analysis for the laboratory calibration of the instrument and for field deployment and obtaining a Langley extra-atmospheric irradiance.
D5	Operation and maintenance manual for lunar photometer	12 page PDF detailing operation and maintenance procedures for the lunar photometer.
D6	Lunar spectral irradiance retrieval from the lunar photometer measurements	15-page PDF describing the process for retrieving lunar irradiance from the ground-based observations, including data pre-processing and iterative Langley plot method
D7	ATBD - Lunar spectral irradiance retrieval from the lunar photometer measurements.	45-page PDF describing the process gone through and the fitting quality for the model at the observation wavelengths, for a polarization model and for the interpolation to other wavelengths.
DB-1	Lunar photometer raw data.	Provided as an ASCII file
SW-1	Prototype lunar spectral irradiance retrieval from the lunar photometer (source code and object code).	Code written in C++
DB-2	Database of lunar spectral irradiance measurements.	Provided as ASCII file
D8	Report on the comparison of the lunar spectral irradiance model to	D8

The calibration coefficients for the instrument determined at NPL along with their associated uncertainties are:

executive summary

Spectral Channel	MOON calibration Coefficient	Standard uncertainty	Expanded uncertainty $k = 2$
340 nm Si	5.306×10^{-09}	1.72%	3.44%
380 nm Si	2.227×10^{-09}	1.20%	2.41%
440 nm Si	5.759×10^{-10}	0.97%	1.94%
500 nm Si	4.481×10^{-10}	0.96%	1.91%
675 nm Si	3.205×10^{-10}	0.93%	1.86%
870 nm Si	2.547×10^{-10}	0.91%	1.82%
937 nm Si	2.431×10^{-10}	0.97%	1.95%
1020 nm Si	2.735×10^{-10}	1.05%	2.11%
1020 nm InGaAs	2.119×10^{-10}	1.01%	2.03%
1640 nm InGaAs	4.893×10^{-11}	1.06%	2.11%

Table 1 in D4: Final calibration coefficients and associated uncertainties for the CIMEL lunar photometer

Figure 6: Lunar irradiance project team at Teide Peak, Tenerife

The project was presented at the following meetings

November 2017	GSICS 2nd Lunar Workshop	Xi'an, China
October 2018	NCEO-CEOI Conference	Birmingham, UK
March 2019	STEM for Britain	House of Commons, UK
March 2019	CEOS-WGCV-IVOS	Perth, Australia
May 2019	Polar Aerosol Optical Depth Retreat	Canaan (CT, USA)
May 2019	Living Planet Symposium	Milan, Italy
September 2019	CEOS-WGCV	NPL, UK